IJMOT

INTERNATIONAL JOURNAL OF MICROWAVE AND OPTICAL TECHNOLOGY,

VOL.5 NO.2 MARCH 2010

Analysis of a Folded E-Plane Tee Using Multiple Cavity Modeling Technique

Debendra Kumar Panda[*] and Ajay Chakraborty

[*]School of Electrical Sciences, VIT University,Vellore-632014, E-mail: p.debendra@vit.ac.in
Department Of Electronics and Electrical Communication Engineering,
Indian Institute of Technology, Kharagpur, West Bengal, India-721302, E-mail: bassein@hijili.iitkgp.ernet.in

***Abstract*- A method of moment based analysis of a folded E-plane tee junction has been presented using Multiple Cavity Modeling Technique (MCMT). The E-plane port is folded to provide the reduction in size. Finally attempt has been made to improve the frequency response characteristic of the waveguide circuit by capacitive loading. The proposed circuit has good agreement with the MCMT, CST microwave studio simulated data and measured data.**

***Index Terms*- Folded E-Plane Tee, multiple cavity modeling technique, moment method analysis, global basis functions.**

I. INTRODUCTION

Waveguide Tee-junction problem is as old as the iris and filters. Variation Method, Boundary Element Method, Finite Element method, Full Wave Mode Matching Technique, Moment method, Resonator method and Overlapping T-block Method was used to analyze this structure [1-8]. Sharp [9] proposed an exact method for calculation of the electrical performance of the rectangular waveguide tee junction. Das and Chakraborty [10] were analyzed a folded E-plane Tee-junction, using MCMT. To analyze this structure the piecewise triangular basis function has been used. Further the analyzed structure was not matched to the junction and could be used as an asymmetric power divider.

In this paper effort has been made to make the folded E-plane Tee-junction symmetric on inclusion of a capacitive load to the structure. The structure has been analyzed using MCMT. Further it has been analyzed using global basis function. The MCMT involves in replacing all the apertures and discontinuities of the waveguide structures, with equivalent magnetic current densities so that the given structure can be analyzed using only Magnetic Field Integral Equation (MFIE).Since only the magnetic currents present in the apertures are considered the methodology involves only solving simple magnetic integral equation rather than the complex integral equation involving both the electric and magnetic current densities.

II. FORMULATION OF THEORY

Fig. 1 shows the three dimensional view of the folded E-plane tee and with its cavity modeling and details of region is shown in Fig. 2 which shows that the structures have 3 waveguide regions and 2 cavity region. The interfacing apertures between different regions are replaced by equivalent magnetic current densities (M_1-M_5). The electric field at the aperture is assumed to be

$$\vec{E} = \hat{u}_x \sum_{p=1}^{M} E_p^x e_p^x + \hat{u}_y \sum_{p=1}^{M} E_p^y e_p^y \qquad (1)$$

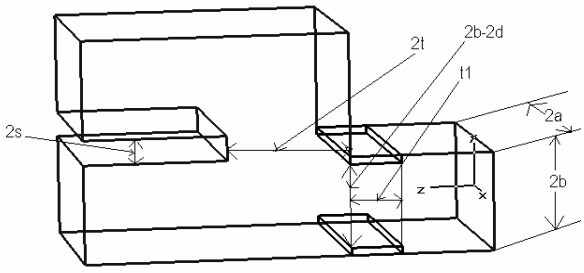

Figure 1: Three dimensional view of a folded E-plane tee with capacitive loading.

Where the basis function e_p (p=1, 2, 3…M) are defined by

$$e_p^{i,y}=\begin{cases}\sin\left\{\dfrac{p\pi}{2L}\left(x-x_w+L\right)\right\} & \text{for } \begin{matrix}x_w\text{-L}\le x\le x_w+L\\ y_w\text{-W}\le y\le y_w+W\end{matrix}\\ 0 & \text{elsewhere}\end{cases} \quad (2)$$

$$e_p^{i,x}=\begin{cases}\sin\left\{\dfrac{p\pi}{2W}\left(y-y_w+W\right)\right\} & \text{for } \begin{matrix}x_w\text{-L}\le x\le x_w+L\\ y_w\text{-W}\le y\le y_w+W\end{matrix}\\ 0 & \text{elsewhere}\end{cases} \quad (3)$$

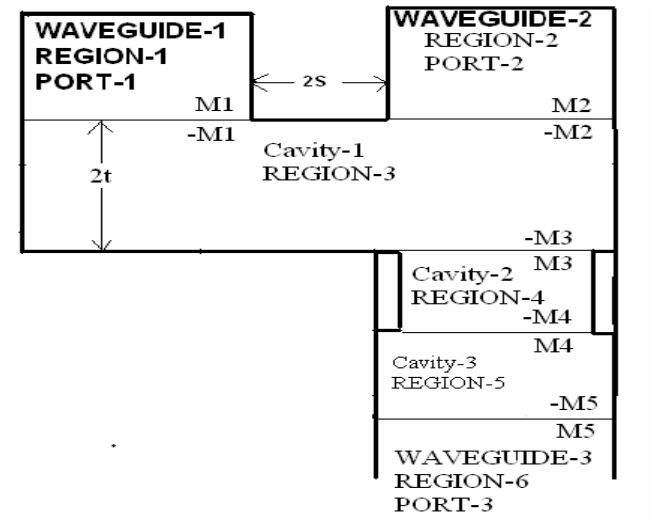

Figure 2: Cavity modeling and details of regions of the folded E-plane tee with capacitive loading.

In the eq. (2) and eq. (3)

- $L=a, W=b$, $x_w=0$ and $y_w=b+s$ for aperture 1 with respect to cavity-1 axis.
- $L=a, W=b$, $x_w=0$ and $y_w=-b-s$ for aperture 2 with respect to cavity-1 axis.
- $L=a, W=b-d$, $x_w=0$ and $y_w=-b-s$ for aperture 3 with respect to cavity-1 axis.
- $L=a, W=b-d$, $x_w=0$ and $y_w=0$ for aperture 3 with respect to cavity-2 axis.
- $L=a, W=b-d$, $x_w=0$ and $y_w=0$ for aperture 4 with respect to cavity-2 axis.
- $L=a, W=b-d$, $x_w=0$ and $y_w=0$ for aperture 4 with respect to cavity-3 axis.
- $L=a, W=b$, $x_w=0$ and $y_w=0$ for aperture 5 with respect to cavity-3 axis.
- Where 2a=22.86 mm, 2b=10.16 mm, s=1.27 mm and d=.78 mm.
- 2s=2.54 mm is the distance between waveguide-1 and waveguide-2.
- 2t=12 mm is the cavity length in the z-direction of cavity-1
- t_1=5 mm is the cavity length in the z-direction of cavity-2
- Cavity length in the z-direction of cavity-3 can be chosen to any length.

The X-component of incident magnetic field at the aperture for the transmitting mode is a dominant TE_{10} mode and is given by

$$H_x^{inc}=-Y_0\cos\left(\frac{\pi x}{2a}\right)e^{-j\beta z} \quad (4)$$

III. EVALUATION OF THE INTERNALLY SCATTERED FIELD

The internally scattered field in the waveguide is obtained by using the modal expansion approach presented in [11]. The internally scattered electric field is given in [12]. Once the electric field is obtained, the corresponding magnetic fields can be derived.

The x-component of internally scattered magnetic field can be obtained as,

$$H_x^{wvg}\left(E_p^{i,y}\right)=H_x^{wvg}\left(M_p^{i,x}\right)$$

$$=\begin{cases}-\sum_{m=1}^{\infty}Y_{m0}^{e}\sin\left\{\dfrac{m\pi}{2a}\left(x+a\right)\right\} & \text{for p = m and n = 0}\\ 0 & \text{Otherwise}\end{cases} \quad (5)$$

$$H_x^{wvg}\left(E_p^{i,x}\right)=-H_x^{wvg}\left(M_p^{i,y}\right)=0 \quad (6)$$

$$H_y^{wvg}\left(E_p^{i,y}\right)=H_y^{wvg}\left(M_p^{i,x}\right)=0 \quad (7)$$

$$H_y^{wvg}\left(E_p^{i,x}\right) = -H_y^{wvg}\left(M_p^{i,y}\right)$$
$$= \begin{cases} \sum_{n=0}^{\infty} Y_{0n}^{e} \sin\left\{\frac{n\pi}{2b}(y+b)\right\} & \text{for p = n and m = 0} \\ 0 & \text{Otherwise} \end{cases} \quad (8)$$

IV. EVALUATION OF THE CAVITY SCATTERED FIELD

The tangential components of the cavity scattered fields are given in [14] where, L_{cj} is the length and W_{cj} is the height of j^{th} the cavity. L_i and W_i are the half length and half width of i^{th} aperture.

$$H_x^{cav^j}\left(M_1^x\right) = -\frac{j\omega\varepsilon}{k^2}\sum_{m=1}^{\infty}\sum_{n=0}^{\infty}\frac{\varepsilon_m\varepsilon_n L_i W_i}{2L_{cj}W_{cj}}\left\{k^2-\left(\frac{n\pi}{2L_c}\right)^2\right\}\sin\left\{\frac{m\pi}{2L_{cj}}(x+L_{cj})\right\}$$
$$\times\cos\left\{\frac{n\pi}{2W_{cj}}(y+W_{cj})\right\}\cos\left\{\frac{n\pi}{2W_{cj}}(y_w+W_{cj})\right\}\mathrm{sinc}\left\{\frac{n\pi}{2W_{cj}}W_i\right\}F_x(p)\times$$
$$\frac{(-1)}{\Gamma_{mn}\sin\{2\Gamma_{mn}t_c\}}\begin{cases}\cos\{\Gamma_{mn}(z-t_c)\}\cos\{\Gamma_{mn}(z_0+t_c)\} & z>z_0\\ \cos\{\Gamma_{mn}(z_0-t_c)\}\cos\{\Gamma_{mn}(z+t_c)\} & z<z_0\end{cases} \quad (9)$$

$$H_x^{cav^j}\left(M_1^y\right) = \frac{j\omega\varepsilon}{k^2}\sum_{m=1}^{\infty}\sum_{n=0}^{\infty}\frac{\varepsilon_m\varepsilon_n L_i W_i}{2L_{cj}W_{cj}}\frac{m\pi}{2L_{cj}}\frac{n\pi}{2W_{cj}}\sin\left\{\frac{m\pi}{2L_{cj}}(x+L_{cj})\right\}\times$$
$$\cos\left\{\frac{n\pi}{2W_{cj}}(y+W_{cj})\right\}\cos\left\{\frac{m\pi}{2L_{cj}}(x_w+L_{cj})\right\}\mathrm{sinc}\left\{\frac{m\pi}{2L_{cj}}L_i\right\}F_y(p)\times$$
$$\frac{(-1)}{\Gamma_{mn}\sin\{2\Gamma_{mn}t_c\}}\begin{cases}\cos\{\Gamma_{mn}(z-t_c)\}\cos\{\Gamma_{mn}(z_0+t_c)\} & z>z_0\\ \cos\{\Gamma_{mn}(z_0-t_c)\}\cos\{\Gamma_{mn}(z+t_c)\} & z<z_0\end{cases} \quad (10)$$

$$H_y^{cav^j}\left(M_1^x\right) = \frac{j\omega\varepsilon}{k^2}\sum_{m=1}^{\infty}\sum_{n=0}^{\infty}\frac{\varepsilon_m\varepsilon_n L_i W_i}{2L_{cj}W_{cj}}\frac{n\pi}{2L_{cj}}\frac{n\pi}{2W_{cj}}\cos\left\{\frac{m\pi}{2L_{cj}}(x+L_{cj})\right\}\times$$
$$\sin\left\{\frac{n\pi}{2W_{cj}}(y+W_{cj})\right\}\cos\left\{\frac{n\pi}{2W_{cj}}(y_w+W_{cj})\right\}\mathrm{sinc}\left\{\frac{n\pi}{2W_{cj}}W_i\right\}F_x(p)\times$$
$$\frac{(-1)}{\Gamma_{mn}\sin\{2\Gamma_{mn}t_c\}}\begin{cases}\cos\{\Gamma_{mn}(z-t_c)\}\cos\{\Gamma_{mn}(z_0+t_c)\} & z>z_0\\ \cos\{\Gamma_{mn}(z_0-t_c)\}\cos\{\Gamma_{mn}(z+t_c)\} & z<z_0\end{cases} \quad (11)$$

$$H_y^{cav^j}\left(M_1^y\right) = -\frac{j\omega\varepsilon}{k^2}\sum_{m=1}^{\infty}\sum_{n=0}^{\infty}\frac{\varepsilon_m\varepsilon_n L_i W_i}{2L_{cj}W_{cj}}\left\{k^2-\left(\frac{n\pi}{2W_{cj}}\right)^2\right\}\cos\left\{\frac{m\pi}{2L_{cj}}(x+L_{cj})\right\}$$
$$\times\sin\left\{\frac{n\pi}{2W_{cj}}(y+W_{cj})\right\}\cos\left\{\frac{m\pi}{2L_{cj}}(x_w+L_{cj})\right\}\mathrm{sinc}\left\{\frac{m\pi}{2L_{cj}}L_i\right\}F_y(p)\times$$
$$\frac{(-1)}{\Gamma_{mn}\sin\{2\Gamma_{mn}t_c\}}\begin{cases}\cos\{\Gamma_{mn}(z-t_c)\}\cos\{\Gamma_{mn}(z_0+t_c)\} & z>z_0\\ \cos\{\Gamma_{mn}(z_0-t_c)\}\cos\{\Gamma_{mn}(z+t_c)\} & z<z_0\end{cases} \quad (12)$$

Where t_c is half length of the cavity in z-direction and Γ_{mn} is the propagation constant.

$$\Gamma_{mn} = \sqrt{k^2-\left(\frac{m\pi}{2l}\right)^2-\left(\frac{n\pi}{2w}\right)^2}.$$

$$k = \omega\sqrt{\mu\varepsilon}$$

$$\varepsilon_i = \begin{cases}1, & \text{i=0}\\ 2, & \text{i}\neq 0\end{cases}$$

$$F_x(p) = \left[\cos\left\{\frac{\pi}{2}\left(-\frac{mx_w}{a_i}+p-m\right)\right\}\sin c\left\{\frac{\pi L}{2}\left(\frac{p}{L}-\frac{m}{a_i}\right)\right\}\right.$$
$$\left.+\cos\left\{\frac{\pi}{2}\left(\frac{mx_w}{a_i}+p+m\right)\right\}\sin c\left\{\frac{\pi L}{2}\left(\frac{p}{L}+\frac{m}{a_i}\right)\right\}\right]$$

and

$$F_y(p) = \left[\cos\left\{\frac{\pi}{2}\left(-\frac{ny_w}{b_i}+p-n\right)\right\}\sin c\left\{\frac{\pi W}{2}\left(\frac{p}{W}-\frac{n}{b_i}\right)\right\}\right.$$
$$\left.+\cos\left\{\frac{\pi}{2}\left(\frac{ny_w}{b_i}+p-n\right)\right\}\sin c\left\{\frac{\pi W}{2}\left(\frac{p}{W}+\frac{n}{b_i}\right)\right\}\right]$$

At the region of the window, the tangential component of the magnetic field in the aperture should be identical and applying the proper boundary conditions at the aperture the electric fields can be evaluated .

V. IMPOSITION OF THE BOUNDARY CONDITION

At the region of the window, the tangential component of the magnetic field in the aperture should be identical and is given by:

Aperture -1, Region-1

$$H_x^{wvg1}\left(M_1^x\right)+H_x^{cav1}\left(M_1^x\right)+H_x^{wvg1}\left(M_1^y\right)+$$
$$H_x^{cav1}\left(M_1^y\right)+H_x^{cav1}\left(M_2^x\right)+H_x^{cav1}\left(M_2^y\right)- \quad (13)$$
$$H_x^{cav1}\left(M_3^x\right)-H_x^{cav1}\left(M_3^y\right) = 2H_x^{inc}$$

$$H_y^{wvg1}\left(M_1^x\right)+H_y^{cav1}\left(M_1^x\right)+H_y^{wvg1}\left(M_1^y\right)+$$
$$H_y^{cav1}\left(M_1^y\right)+H_y^{cav1}\left(M_2^x\right)+H_y^{cav1}\left(M_2^y\right)- \quad (14)$$
$$H_y^{cav1}\left(M_3^x\right)-H_y^{cav1}\left(M_3^y\right) = 0$$

Aperture -2, Region-2

$$\begin{aligned}&H_x^{cav1}(M_1^x)+H_x^{cav1}(M_1^y)+H_x^{cav1}(M_2^x)+\\&H_x^{wav2}(M_2^x)+H_x^{cav1}(M_2^y)+H_x^{wav-2}(M_2^y)-\\&H_x^{cav1}(M_3^x)-H_x^{cav1}(M_3^y)=0\end{aligned} \quad (15)$$

$$\begin{aligned}&H_y^{cav1}(M_1^x)+H_y^{cav1}(M_1^y)+H_y^{cav1}(M_2^x)+\\&H_y^{wav2}(M_2^x)+H_y^{cav1}(M_2^y)+H_y^{wav2}(M_2^y)-\\&H_y^{cav1}(M_3^x)-H_y^{cav1}(M_3^y)=0\end{aligned} \quad (16)$$

Aperture -3, Region-2

$$\begin{aligned}&-H_x^{cavl}(M_1^x)-H_x^{cavl}(M_1^y)-H_x^{cavl}(M_2^x)-H_x^{cavl}(M_2^y)+\\&H_x^{cavl}(M_3^x)+H_x^{cav2}(M_3^x)+H_x^{cavl}(M_3^y)+H_x^{cav2}(M_3^y)-\\&H_x^{cav2}(M_4^x)-H_x^{cav2}(M_4^y)=0\end{aligned} \quad (17)$$

$$\begin{aligned}&-H_y^{cavl}(M_1^x)-H_y^{cavl}(M_1^y)-H_y^{cavl}(M_2^x)-H_y^{cavl}(M_2^y)+\\&H_y^{cavl}(M_3^x)+H_y^{cav2}(M_3^x)+H_y^{cavl}(M_3^y)+H_y^{cav2}(M_3^y)-\\&H_y^{cav2}(M_4^x)-H_y^{cav2}(M_4^y)=0\end{aligned} \quad (18)$$

Aperture -4, Region-3

$$\begin{aligned}&-H_x^{cav2}(M_3^x)-H_x^{cav2}(M_3^y)+H_x^{cav2}(M_4^x)+\\&H_x^{cav3}(M_4^x)+H_x^{cav2}(M_4^y)+H_x^{cav3}(M_4^y)-\\&H_x^{cav3}(M_5^x)-H_x^{cav3}(M_5^y)=0\end{aligned} \quad (19)$$

$$\begin{aligned}&-H_y^{cav2}(M_3^x)-H_y^{cav2}(M_3^y)+H_y^{cav2}(M_4^x)+\\&H_y^{cav3}(M_4^x)+H_y^{cav2}(M_4^y)+H_y^{cav3}(M_4^y)-\\&H_y^{cav3}(M_5^x)-H_y^{cav3}(M_5^y)=0\end{aligned} \quad (20)$$

Aperture -5, Region-4

$$\begin{aligned}&-H_x^{cav3}(M_4^x)-H_x^{cav3}(M_4^y)+H_x^{cav3}(M_5^x)+\\&H_x^{wav3}(M_5^x)+H_x^{cav3}(M_5^y)+H_x^{wav3}(M_5^y)=0\end{aligned} \quad (21)$$

$$\begin{aligned}&-H_y^{cav3}(M_4^x)-H_y^{cav3}(M_4^y)+H_y^{cav3}(M_5^x)+\\&H_y^{wav3}(M_5^x)+H_y^{cav3}(M_5^y)+H_y^{wav3}(M_5^y)=0\end{aligned} \quad (22)$$

VI. SOLVING FOR THE ELECTRIC FIELD

To determine the electric field distribution at the window aperture, it is necessary to determine the basis function coefficients $E_p^{i,x/y}$ at both the apertures. Since the each component of the field is described by M basis functions, 10M unknowns are to be determined from the boundary conditions. The Galerkin's specialization of the method of moments is used to obtain 10M-different equations from the boundary condition to enable determination of $E_p^{i,x/y}$ [13]. The weighting function $w_q^{i,x/y}(x,y,z)$ is selected to be of the same form as the basis function $e_p^{i,x/y}$. The weighting function is defined as follows:

$$w_q^{i,y}=\begin{cases}\sin\left\{\dfrac{q\pi}{2L}(x-x_w+L)\right\} & \text{for } \begin{matrix}x_w\text{-L}\le x\le x_w+L\\ y_w\text{-W}\le y\le y_w+W\end{matrix}\\ 0 & \text{elsewhere}\end{cases} \quad (23)$$

$$w_q^{i,x}=\begin{cases}\sin\left\{\dfrac{q\pi}{2W}(y-y_w+W)\right\} & \text{for } \begin{matrix}x_w\text{-L}\le x\le x_w+L\\ y_w\text{-W}\le y\le y_w+W\end{matrix}\\ 0 & \text{elsewhere}\end{cases} \quad (24)$$

The inner product is defined by

$$\langle H,w_q\rangle=\iint_{Aperture} H\bullet w_q\,dxdy \quad (25)$$

Where the elements of the moment matrices are derived as follows:

$$\langle H_x^{inc},w_q^{1,y}\rangle=\begin{cases}-2abY_0 & \text{for q = 1}\\ 0 & \text{Otherwise}\end{cases} \quad (26)$$

$$\langle H_x^{wvg}(M_x),w_q^{i,y}\rangle=\begin{cases}-2abY_{m0}^e & \text{for p = q = m and n = 0}\\ 0 & \text{Otherwise}\end{cases} \quad (27)$$

$$\langle H_x^{wvg}(M_y),w_q^{i,y}\rangle=0 \quad (28)$$

$$\langle H_y^{wvg}(M_x),w_q^{i,x}\rangle=0 \quad (29)$$

$$\langle H_y^{wvg}(M_y),w_q^{i,x}\rangle=\begin{cases}-2abY_{0n}^e & \text{for p = q = n and m = 0}\\ 0 & \text{Otherwise}\end{cases} \quad (30)$$

$$\begin{aligned}&\langle H_x^{wvg}(M_x),w_q^{i,y}\rangle=\\&-\frac{j\omega\varepsilon}{k^2}\frac{L_sW_sL_bW_o}{2L_cW_c}\sum_{m=1}^{\infty}\sum_{n=0}^{\infty}\varepsilon_m\varepsilon_n\left\{k^2-\left(\frac{n\pi}{2L_c}\right)^2\right\}\times\\&\cos\left\{\frac{n\pi}{2W_c}(y_{ws}+W_c)\right\}\operatorname{sinc}\left\{\frac{n\pi}{2W_c}W_s\right\}\cos\left\{\frac{n\pi}{2W_c}(y_{wo}+W_c)\right\}\operatorname{sinc}\left\{\frac{n\pi}{2W_c}W_o\right\}\times\\&\frac{\{-F_{xs}(p)F_{xo}(q)\}}{\Gamma_{mn}\sin\{2\Gamma_{mn}t_c\}}\begin{cases}\cos\{\Gamma_{mn}(z-t_c)\}\cos\{\Gamma_{mn}(z_0+t_c)\} & z\ge z_0\\ \cos\{\Gamma_{mn}(z_0-t_c)\}\cos\{\Gamma_{mn}(z+t_c)\} & z\le z_0\end{cases}\end{aligned} \quad (31)$$

where suffix 's' and 'o' represents the source and observation aperture dimensions respectively.

VII. REFLECTION COEFFICIENT AND TRANSMISSION COEFFICIENT

To determine the reflection coefficient, we decouple the sources, one at $-\infty$ in the feed waveguide and the other at the window. The incident electric field due to the TE_{10} excitation at the z = 0 plane is,

$$E_y^{inc} = \cos\left(\frac{\pi x}{2a_i}\right) \tag{32}$$

When the window aperture is shorted, the electric field is the field reflected by the electric short circuit and is given by,

$$E_y^1 = -\cos\left(\frac{\pi x}{2a_i}\right) \tag{37}$$

When the generator in the feed waveguide is removed and replaced by a perfect match, the electric field for the dominant TE_{10} mode scattered by the window into the waveguide is derived from equation (36) by substituting m =1, n = 0, at the z = 0 plane as:

$$E_y^2 = \sum_{p=1}^{M} E_p^{i,y} \frac{WL}{ab}\left[\cos\left\{\frac{\pi}{2}\left(-\frac{x_w}{a}+p+1\right)\right\}\sin c\left\{\frac{\pi L}{2}\left(\frac{p}{L}-\frac{1}{a}\right)\right\} - \cos\left\{\frac{\pi}{2}\left(\frac{x_w}{a}+p+1\right)\right\}\sin c\left\{\frac{\pi L}{2}\left(\frac{p}{L}+\frac{1}{a}\right)\right\}\right]\cos\left(\frac{\pi x}{2a}\right) \tag{38}$$

Reflection coefficient Γ can then be expressed as:

$$\Gamma = \frac{E_y^1+E_y^2}{E_y^{inc}} = -1+\frac{WL_i}{a_i b_i}\sum_{p=1}^{M} E_p^{i,y}\left[\cos\left\{\frac{\pi}{2}\left(-\frac{x_w}{a_i}+p+1\right)\right\}\sin c\left\{\frac{\pi L_i}{2}\left(\frac{p}{L_i}-\frac{1}{a_i}\right)\right\} - \cos\left\{\frac{\pi}{2}\left(\frac{x_w}{a_i}+p+1\right)\right\}\sin c\left\{\frac{\pi L_i}{2}\left(\frac{p}{L_i}+\frac{1}{a_i}\right)\right\}\right] \tag{39}$$

The transmission coefficient is given by

$$T_{ji} = \frac{E_y^{transmitted}}{E_y^{inc}} = \frac{WL_j}{a_j b_j}\sum_{p=1}^{M} E_p^{i,y}\left[\cos\left\{\frac{\pi}{2}\left(-\frac{x_w}{a_j}+p+1\right)\right\}\sin c\left\{\frac{\pi L_j}{2}\left(\frac{p}{L_j}-\frac{1}{a_j}\right)\right\} - \cos\left\{\frac{\pi}{2}\left(\frac{x_w}{a_j}+p+1\right)\right\}\sin c\left\{\frac{\pi L_j}{2}\left(\frac{p}{L_j}+\frac{1}{a_j}\right)\right\}\right] \tag{40}$$

The scattering matrix for this folded E-plane tee is as follows:

$$\begin{pmatrix} S_{11} & S_{12} & S_{13} \\ S_{21} & S_{22} & S_{23} \\ S_{31} & S_{32} & S_{33} \end{pmatrix} \tag{41}$$

VIII. NUMERICAL RESULTS AND DISCUSSION

Theoretical data for the magnitude of scattering parameters for folded E-plane Tee at X-band has been compared with CST Microwave Studio simulated data and measured data.

MATLAB codes have been written for analyzing the structure and numerical data have been obtained after running the codes. The structure was also simulated using CST microwave studio while measurements were performed using Agilent 8410C Vector Network Analyzer. The theory has been validated by the excellent agreement between the CST Microwave Studio simulated data and Measured Data.

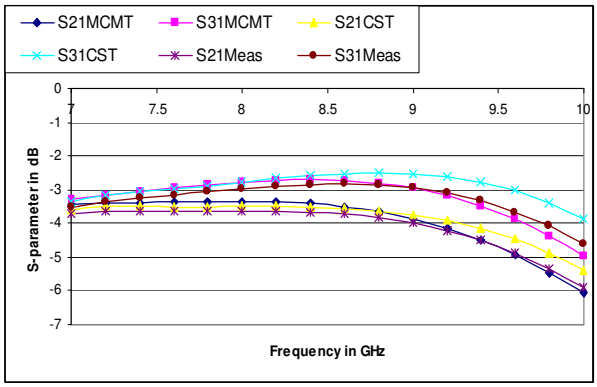

Figure 3: Comparison of MCMT, CST Microwave Studio simulated and measured data for S-Parameter of a folded E-Plane Tee without Capacitive loading at port-3 for 2t=12mm when excited at port-1.

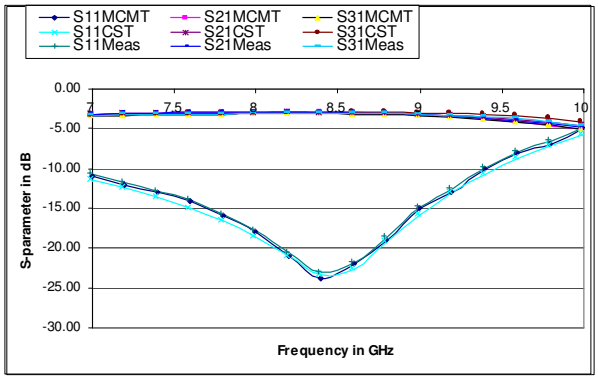

Figure 4: Comparison of MCMT, CST Microwave Studio simulated and measured data for S-Parameter of a folded E-Plane Tee with Capacitive loading at port-3 for 2t=12mm when excited at port-1.

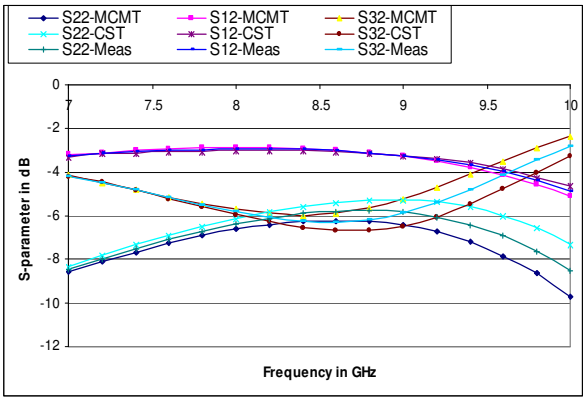

Fig 5: Comparison of MCMT, CST Microwave Studio simulated and measured data of S-Parameter of a folded E-Plane Tee with Capacitive loading at port-3 for 2t=12mm when excited at port-2.

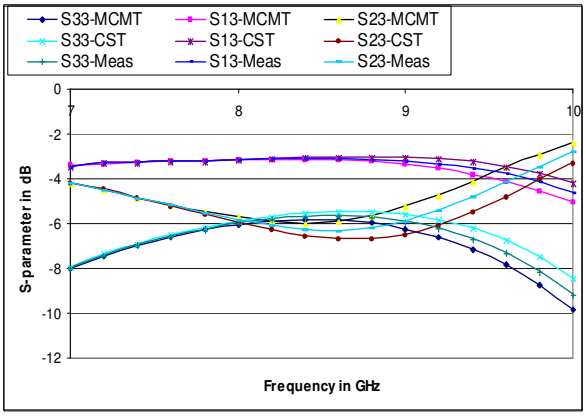

Fig 6: Comparison of MCMT, CST Microwave Studio simulated and measured data of S-Parameter of a folded E-Plane Tee with Capacitive loading at port-3 for 2t=12mm when excited at port-3.

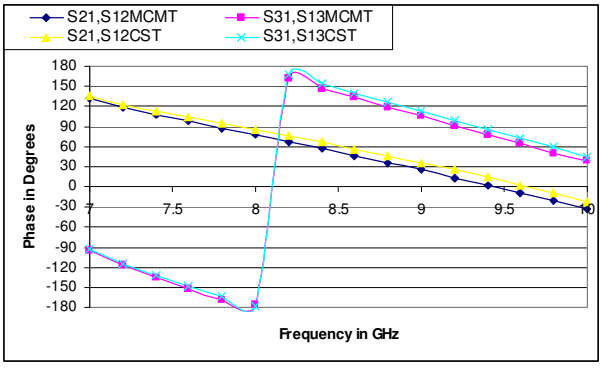

Figure-7: Comparison of MCMT and CST Microwave Studio simulated data for phase of S-Parameter S21, S12, S13, and S31 of a folded E-Plane Tee with 2t=12 mm.

Fig. 3 shows the S-parameters for the proposed folded E-plane tee without capacitive loading. In Fig. 4 to Fig. 6 the magnitude of S-parameters for the proposed folded E-plane Tee has been shown, which shows that the $S_{21,}$ $S_{12,}$ S_{13} and S_{31} have the equal magnitude of near about -3dB at the frequency range 7-9 GHz. In Fig. 7, the phase of the $S_{21,}$ $S_{12,}$ S_{13} and S_{31} have shown. The Measured data for phase analysis has not been shown in Fig.7, being it is completely different from the computed data. The reason of this difference is, in the mathematical modeling, the E plane band arrangements are not included what is used for measurement purposes.

IX. CONCLUSION

The result shown in Fig. 3 depicts that the folded E-plane Tee junctions are not matched to the junctions for equal power division. The inclusion of capacitive loading to port-3 makes the junction matched and equal power division can be achieved over the frequency range of 7-9 GHz. Folding the E-plane arm gives compactness to the structure. Furthermore, it can be tuned to other band of frequency by changing the iris dimensions.

ACKNOWLEDGMENT

The support provided by Kalpana Chawla Space Technology Cell, IIT Kharagpur is gratefully acknowledged..

REFERENCES

[1] B. N. Das, P.V.D.S. Rao, A Chakraborty, "**Analysis of T-junction Between Rectangular to Circular Waveguides by Variational Method"** Proc. IEE, Part-H, Vol-13,No-6, pp. 475-479,1989.

[2] Y. H. Cho, "**Analysis of an *E*-plane waveguide T-junction with a quarter-wave transformer using the overlapping T-block method and genetic algorithm**," Microwaves, Antennas and Propagation, IEE Proceedings, Vol. 151, Issue 6, pp.503 – 506, 19 Dec. 2004.

[3] T. Obata and J. Chiba, "**Improved Theory for E-Plane Symmetrical Tee Junctions**," IEEE Transactions on Microwave Theory and Techniques, Vol. MTT-37, No. 3, pp. 624-627, March 1989.

[4] X. P. Liang, K. A. Zaki and A. E. Atia, "**A Rigorous Three Plane Mode-Matching Technique for Characterizing Waveguide T-Junctions, and its**

Application in Multiplexer Design," IEEE Transactions on Microwave Theory and Techniques, Vol. MTT-39, No. 12, pp. 2138-2147, December 1991.

[5] P. Lampariello and A. Oliner, "**New Equivalent Networks with Simple Closed-Form Expressions for Open and Slit-Coupled E-Plane Tee Junctions**," IEEE Transactions on Microwave Theory and Techniques, Vol. MTT-41, No. 5, pp. 839-847, May 1993.

[6] H. W. Yao, A. Liang. Abdelmonem, J. H., X. P. Liang and K. A. Zaki, "**Waveguide and Ridge Waveguide T-Junctions for Wide Band Applications**," Microwave Symposium Digest, 1993., IEEE MTT-S International, Vol.2, pp. 601 – 604, 14-18 June 1993.

[7] C. Wang and K. A. Zaki, "**Full-Wave Modeling of Generalized Double Ridge Waveguide T-Junction,**" IEEE Transactions on Microwave Theory and Techniques, Vol. MTT-44, No. 12, pp. 2536-2542, December 1996.

[8] C. O. Lee, C. C. Shin, S. T. Kim, K. H. Ra and Y. C. Lee, "**The Modified Stepped Waveguide T-Junctions and the Method of Initial Design**," Asia-Pacific Microwave Conference, pp. 388-391, 3-6 December, 2000.

[9] E. D. Sharp, "**An Exact Calculation for a T-Junction of Rectangular Waveguides Having Arbitrary Cross Sections,**" IEEE Transactions on Microwave Theory and Techniques, Vol. MTT-15, No. 2, pp. 109-116, February 1967.

[10] S. Das, A. Chakrabarty and A. Chakraborty "**Analysis Of Folded E-Plane Tee Junction Using Multiple Cavity Modeling Technique**," ICECE 2006, Dhaka, Bangladesh

[11] Harrington, R.F., "Time-Harmonic Electromagnetic Fields", McGraw-Hill Book Company, New York, 1961.

[12] S. Das and A. Chakrabarty, "**A Novel Modeling Technique to Solve a Class of Rectangular Waveguide Based Circuits and Radiators,**" Progress in Electromagnetic Research, MIT, USA, Vol. 61, pp. 231-252, May 2006.

[13] R.F. Harrington, **"Field Computation by Moment Methods"**, Roger E. Krieger Publishing Company, USA

[14] D. K. Panda and A. Chakraborty, "Analysis of a 1:2 Rectangular Waveguide Power Divider for Phased Array Application Using Multiple Cavity Modeling Technique", Progress In Electromagnetic Research Symposium,2008, Cambridge, USA, pp361-368.